

X-Band Reconfigurable Phase Shifters Based on SIW and Liquid Metal Technologies

Shaker Alkaraki¹, Quan Wei Lin², Syeda Fizzah Jilani³, Hang Wong², Alejandro L. Borja⁴, Shiyang Tang⁵, Yi Wang⁶, James R. Kelly⁷

¹ George Green Institute for Electromagnetic Research, Department of Electrical and Electronic Engineering, University of Nottingham, Nottingham NG7 2RD, U.K

²The State Key Laboratory of Terahertz Millimeter Waves, City University of Hong Kong, Hong Kong

³Department of Physics, Physical Sciences Building, Aberystwyth University, Aberystwyth, U.K, SY23 3BZ

⁴Escuela de Ingenieros Industriales, Universidad de Castilla-La Mancha, 02071 Albacete, Spain.

⁵Electronic and Computer Science, University of Southampton, Southampton, U.K, SO17 1BJ

⁶School of Engineering, University of Birmingham, Birmingham, U.K, B15 2TT

⁷School of Electronic Engineering and Computer Science, Queen Mary University of London, London E1 4NS, U.K

Shaker.Alkaraki@nottingham.ac.uk

Abstract — This paper presents three reconfigurable phase shifters operate at X-band and designed utilizing liquid metal (LM). The phase shifters operate at 10 GHz and they have very low insertion loss performance and able to handle high levels of radio frequency (RF) power. Besides, the proposed phase shifters able to achieve a total of 360° phase shift and they are compact in size as they are designed using substrate integrated waveguides (SIW). This enable the proposed phase shifters to be integrated within SIW based feeding structures to realize complete phased array antenna systems. The phase shift is realized by inserting a series of liquid metal vias in the SIW. When a single or multiple via connection is needed, the via hole is filled with liquid metal and conversely, the liquid metal is withdrawn from the via when the connection is no longer required.

Keywords — phase shifter, Gallium, reconfigurable devices, phased array, SIW.

I. INTRODUCTION

Different Radio Frequency (RF) systems, including microwave instrumentation, electronically steerable antennas, and advanced smart antennas, rely on using phase shifters. However, phase shifters employed in microwave frequency ranges have several limitation including that they suffer from high insertion losses (IL). These phase shifters have traditionally been crafted using diverse methodologies, such as: the utilization of 90° hybrid couplers, switched transmission lines, periodic loaded lines, and uneven-length, unequal-width transmission lines. While these techniques offer high phase-shifting capabilities and overall reasonable performance, their considerable physical dimensions remains one of their drawbacks [1].

Among the phase shifter designs frequently employed are those constructed around PIN diodes and GaAs FETs. GaAs FET-based phase shifters provide reduced IL, but face restrictions regarding their ability to manage radio frequency

(RF) power. However, phase shifters based on PIN diodes are able to handle relatively higher RF power levels but are they have relatively poor IL performance [2]-[3].

A different adopted approach to realize phase shifters involves the application of CMOS technology. CMOS enables precise resolution and accuracy within a compact form factor suitable for integration into integrated circuits (ICs). Moreover, CMOS-based phase shifters introduce several disadvantages, including amplitude degradation, constrained RF output power, and relatively poor noise characteristics. This is due to their high insertion losses and nonlinear behaviour. In more detail, a state-of-the-art CMOS-driven active phase shifter frequently exhibits an IL performance surpassing 10 dB at 10 GHz [1], [4].

Liquid Crystal and Ferroelectric Ceramics are among other technologies which has been adopted to realize phase shifters. However, the adoption of Ferroelectric phase shifters has been relatively constrained, primarily due to issues associated with their manufacturing, high IL, and limited phase-shifting capabilities. An example of these is a Ferroelectric phase shifter featured in [5] operate at 10GHz and exhibits an IL of 6.6 dB and achieves a phase shift of 342°. Besides, the Ferroelectric-based phase shifter described in [6] records an IL of 10.3 dB at the same frequency band.

In recent times, there has been a surge in interest regarding the utilization of Gallium-based Liquid Metal (LM) for the creation of adaptable circuits and microwave devices. This trend extends to a diverse range of applications, including: microwave filters, RF, switches, antennas, and phase shifters [7]-[14].

This paper introduces three phase shifters that can be modified through the application of LM and are well-suited for incorporation into a phased array system. These phase shifters offering a remarkable tuning range of up to 360°, while simultaneously maintaining exceptionally low insertion loss (IL). Also, the proposed phase shifters have compact electrical footprint. Other advantages of the proposed phase shifters

include their capability of handling high RF power capability and their ability to be integrated in a feeding structure based on substrate integrated waveguides (SIW) to build phased array antenna.

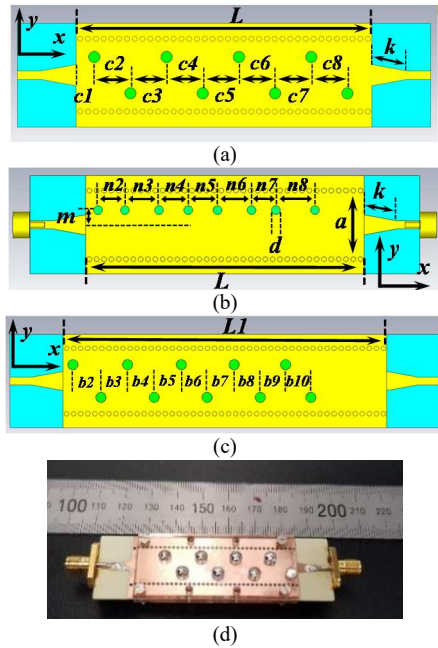


Fig. 1. The schematics of the proposed phase shifters. (a) Alternating liquid metal (LM) vias with 8 vias, (b) non-alternating LM vias with 8 vias and 45° phase step, and (c) alternating LM vias with 10 vias and 36° phase step and (d) prototype of the phase shifter with 8 alternating vias. [dimensions: $a = 14\text{mm}$, $m = 3\text{mm}$, $n2 = 5.5\text{ mm}$, $n3 = 7\text{mm}$, $n4 = 6\text{mm}$, $n5 = 6.1\text{mm}$, $n6 = 7\text{mm}$, $n7 = 5.2\text{mm}$, $n8 = 7.9\text{mm}$, $d = 1.8\text{mm}$, $k = 6.8\text{mm}$, $L = 57.2\text{mm}$, $c1 = 2.6\text{mm}$, $c2 = 6.7\text{ mm}$, $c3 = 5.7\text{ mm}$, $c4 = 6.2$, $c5 = 6.1$, $c6 = 6\text{mm}$, $c7 = 6.3\text{ mm}$, $c8 = 6.2\text{mm}$, $L1 = 67.7\text{mm}$, $l = 3.5\text{mm}$, $b2 = 6\text{mm}$, $b3 = 5.7\text{mm}$, $b4 = 5.7\text{mm}$, $b5 = 6.8\text{mm}$, $b6 = 5.5\text{mm}$, $b7 = 5.8\text{mm}$, $b8 = 5.6\text{mm}$, $b9 = 5.4\text{mm}$, $b10 = 5.4\text{ mm}$].

II. CONCEPT AND STRUCTURE

A phase shift can be achieved when employing a high-pass filter within a topology referred to as a switched high-pass/low-pass [15]-[17]. This filter can be implemented using various technologies, one of which is involving a cylindrical conductive post or an array of such posts within a standard rectangular or circular waveguide. This conductive post in the waveguide is analogous to a via in an SIW transmission line. Both the horizontal position of the post and its diameter serve as parameters for controlling the achieved phase shift. Furthermore, a high-pass filter composed of a T-network of several lumped elements is a feasible representation of a single metal post inside the SIW and the waveguide. The phase shift (φ) is modulated by the susceptance (B) and the reactance (X) as in (1) [15]-[17].

$$\varphi = \frac{B + 2X - BX^2}{2(1 - 2BX)} \quad (1)$$

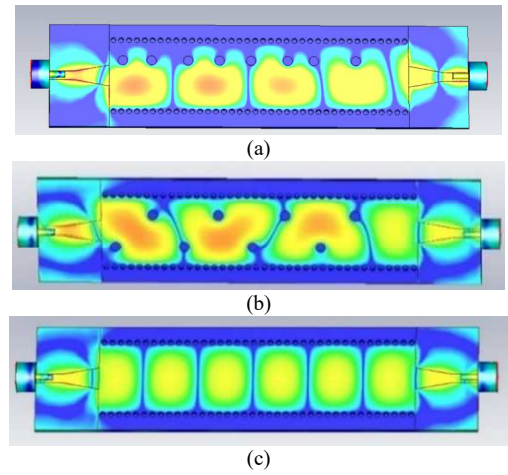


Fig. 2. The electric field inside the SIW for different phase shifters at 10 GHz. (a) Non-alternating LM vias, (b) alternating LM vias, (c) No LM vias.

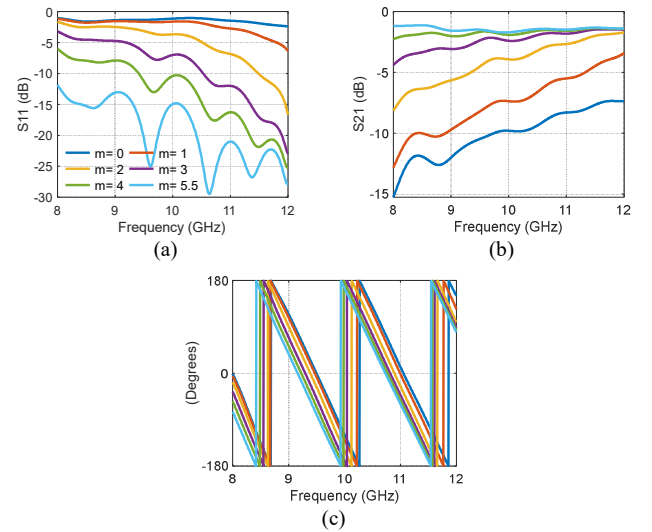


Fig. 3. The effect of first via dimensions m on the performance of the X-band reconfigurable phase shifter. (a) S_{11} , (b) S_{21} and (c) S_{21} phase.

Relying on Eq. 1, we have designed two phase shifters based on SIW technology. These phase shifters are engineered to function at a frequency of 10 GHz, which corresponds to the center frequency of the X-Band. The schematic representation of the proposed phase shifters are in Fig. 1. Our design incorporates several Liquid Metal (LM) vias, each characterized by a specific via diameter denoted as “ d ”. Three phase shifters are proposed. The first phase shifter (Phase shifter A) is with series of eight alternating LM vias as shown in Fig. 1(a) and the second phase shifter (phase shifter B) is with a series of eight non-alternating LM vias as shown in Fig. 1 (b). However, the third phase shifter (phase shifter C) is with ten alternating LM vias. All phase shifters are implemented employing SIW technology using a RO4003C substrate, which possesses a thickness measuring 0.813mm. The substrate exhibits a tangent loss of 0.0027 and a dielectric constant of 3.55.

Indeed, the introduction of a single via into an SIW transmission line induces a phase shift that varies directly with the diameter and it varies inversely with the distance between

the SIW's center and the via's position along the y-axis (m). LM via causes a phase advance to the electromagnetic (EM) wave propagating within the SIW. In simpler terms, the addition of this via reduces the electrical length of the SIW transmission line, thus shortening the path for the wave and naturally leading to a phase advance in the EM wave. Extending this concept, by incorporating an array of vias, as shown in Fig. 1 and 2. Further reduces the electrical length of the SIW. Consequently, this series of vias amplifies the phase advance, resulting in a more pronounced phase shift that can be finely tuned by adjusting the spacing between the vias along the x-axis. In more detail, the array of vias can be arranged in two different configurations as follows: 1) alternating via configuration as shown in Fig. 1(a) and (c) and 2) non-alternating via configuration as shown in Fig. 1.(b).

Moreover, the control of both phase shift and IL caused by an individual LM via is achieved through precise adjustment of the via's horizontal position along the y-axis, as explained in Fig. 3. The degree of phase shift resulting from each via has an inverse relationship with the parameter m . For example, Each via with diameter of 1.8 mm, one can achieve a phase shift spanning approximately between 5° and 79° , in 1° increments, by gradually varying the value of m from 5.5 mm to 0 mm, as explained in Fig. 3(b).

Furthermore, the IL is directly proportional to the magnitude of phase shift introduced by each via. This increase in IL is caused by mismatch, as shown in Fig. 3(a) and (b). It is important to note that, in order to achieve a higher phase shift per via, the respective via should be repositioned closer to the origin of the y-axis in the SIW transmission line. In more detail, when m is set at 5.5 mm, the IL stands at -1.66 dB, and it incrementally rises as the via moves closer towards the center of the SIW. For instance, when $m = 3$ mm, the insertion loss reaches -2.3 dB; at $m = 2$ mm, the insertion loss is -3.9 dB; and at $m = 0$ mm, the insertion loss reaches -9.8 dB as shown in Fig. 3(b).

In addition, adding a series of vias increases the total phase shift achieved by the phase shifter. However, we found that using alternating positions of the vias as shown in Fig. 1 (a) and (c) achieves much higher total shift and better IL performance in comparison to using non-alternating position shown in Fig. 1(b). For instance, the phase shifter with non-alternating position of the vias only achieves a total phase shift of 265.2° with 8 LM vias. However, the phase shifter with alternating position of vias achieves a total phase shift of $\approx 360^\circ$ with 8 LM vias.

In principle, by using vias formed of liquid metal, it becomes feasible to craft a reconfigurable phase shifter comprising eight or more LM vias, capable of delivering a phase shift of up to 265° when employing non-alternating vias and a total 360° phase shift when alternating vias are used. In more detail, the establishment of a via connection is achieved by introducing LM into the via hole when connectivity is desired, and conversely, the LM is withdrawn from the via when the connection is no longer required. For instance, the phase shifter shown in Fig. 1(a) (Phase shifter A) is capable of achieving a 360° phase shift, operating in nine distinctive states.

In State 1, no LM is present in the vias, resulting in a phase shift of 0° . In State 2, liquid metal is introduced into the first via, resulting in a 45° phase shift. In State 3, liquid metal is inserted within the first two vias, delivering a phase shift of 90° . In State 4, liquid metal is inserted in the first three vias, yielding a total phase shift of 135 degrees. In State 5 liquid metal is inserted in the first four vias, accomplishing a 180° phase shift. Similarly, for all subsequent states, each additional activated via results in a 45° phase increment until reaching 360° when all eight LM vias are activated.

III. DESIGN PROCEDURE

The design procedure for the proposed LM X-band phase shifters is explained below:

a) design an SIW that operate on 10 GHz which is centre of X-band based on the design principles. The cut off frequency of the dominant TE_{10} and TE_{20} modes SIW is determined by the width of the SIW (a) [18]-[19]. For example, the proposed SIW is with $a = 14$ mm. This makes the SIW with lower cutoff frequency of 5.7GHz and with upper cutoff frequency of 11.6GHz.

(b) add the first LM via. The required phase shift is controlled by the distance between the centre of the structure and the centre of the LM via.

(c) add the other subsequent vias to increase the phase shift. In more details:

1) for phase shifter A which the phase shifter with eight alternating vias shown in Fig. 1(a), the dimensions c_2 to c_8 are optimized to achieve $\approx 45^\circ$, so the total phase shift achieved by the phase shifter with 8 vias is $\approx 360^\circ$.

2) for phase shifter B which is the is phase shifter with eight non-alternating vias shown in Fig. 1(b), the dimensions between the eight LM vias n_2 to n_8 are optimized for maximum phase shift per via and hence to obtain the maximum phase shift.

3) for phase shifter C which is the phase shifter with ten alternating vias shown in Fig. 1(c), the dimensions b_2 to b_{10} are optimized to achieve $\approx 36^\circ$, so the total phase shift achieved by the phase shifter with ten LM vias is $\approx 360^\circ$.

IV. RESULTS AND DISCUSSION

The proposed phase shifters are modelled and simulated using CST Microwave Studio. Three different phase shifters are simulated and their performance is compared. The first phase shifter is phase shifter A which is with eight alternating LM vias and it achieves a total phase shift of 360° with a step of 45° . The second phase shifter is phase Shifter B is with eight non-alternating LM vias and it achieves a total phase shift of 265.7° . However, the third phase shifter is phase shifter C which is with ten LM vias and it achieves a total phase shift of 360° with steps of 36° .

A. Phase Shifter A with eight non alternating LM via

The proposed phase shifter offers a variable phase adjustment ranging from 0° to 360° , featuring eight discrete steps depending on the number of active LM vias. Fig. 4 presents the performance characteristics of the proposed phase shifter. When all LM vias are activated, it exhibits a remarkable

phase shift of 368.6° at a frequency of 10 GHz, in comparison to the simulated value of 360.5° . Besides, the phase shifter maintains very good IL performance of less than 2.8 dB, as demonstrated in Fig. 4(b) and in Table I. These findings reveal a high level of agreement between the simulated and measured phase responses. The comprehensive phase and IL results, specifically at 10 GHz, are given in Table I. The measured phase steps are consistently around 45° with some discrepancies in the measured phase. These discrepancies primarily is due fabrication tolerances, notably variations in the position and dimensions of individual via holes. For instance, simulations indicate that a 0.1 mm fabrication error in the m position can lead to a phase shift deviation of more than 2.5° , while a similar error in $c2$ to $c8$ can result in a phase shift discrepancy of up to 2.5° . Finally, the insertion loss of the phase shifter can be primarily attributed to matching and dissipation losses within the substrate.

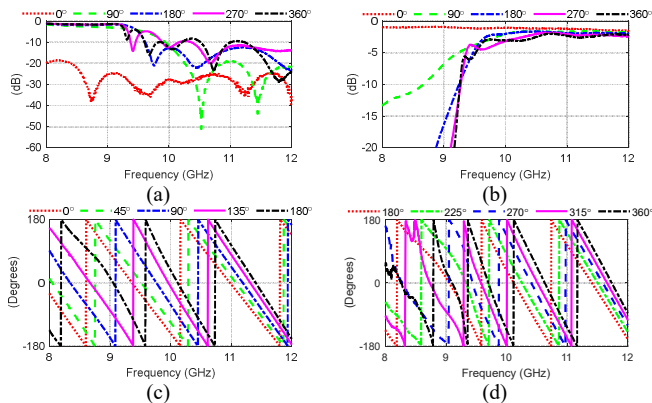


Fig. 4. The measured S_{11} and S_{21} of phase shifter A. (a) S_{11} , (b) amplitude of S_{21} and (c)-(d) S_{21} phase

TABLE I.
SUMMARY OF THE MEASURED AND SIMULATED PERFORMANCE OF PHASE SHIFTER A AT 10 GHz WITH EIGHT ALTERNATING LM VIAS

State (S)	active LM vias	Simulated phases (step)	Measured phases (Step)	Insertion Loss(dB)
(S1)	0	NA	NA	1.7
(S2)	1	30.5° (30.5°)	31.2° (31.2°)	2.3
(S3)	2	77.8° (47.3°)	81.8° (50.6°)	1.9
(S4)	3	125.3° (47.5°)	132.3° (50.5°)	1.9
(S5)	4	172.7° (47.4°)	179° (46.7°)	2.0
(S6)	5	219.5° (46.8°)	223.8° (44.8°)	2.1
(S7)	6	267° (47.5°)	277.9° (53.1°)	2.7
(S8)	7	313.9° (46.9°)	323.4° (46.5°)	2.3
(S9)	8	360.5° (46.6°)	367.6° (44.2°)	2.8
	Total	360.5	367.6	

B. Phase Shifter B with Eight non alternating LM via

The distance, in y-axis direction, between centre of proposed phase shifter and each of the vias (i.e. $m = 4.3$ mm) was configured to be identical to the value of m used in the phase shifter, incorporating alternating vias. This is to compare the performance of both phase shifters. However, the distances between the LM vias (i.e. $n2$ to $n8$), in the new phase shifter, were re-optimized to produce the maximum phase shift per via.

The maximum phase shift that can be achieved using this methodology is 265.2° , as given in Table. II. This is significantly smaller than the maximum phase shift that can be achieved when using alternating vias. Besides, the phase shifter with non-alternating vias has worse insertion loss performance for majority of states. Arranging the vias in a non-alternating manner changes the effective electrical width of the waveguide as shown in Fig. 2(a). The reduction in the width of the waveguide results in a deterioration of the matching performance of the phase shifter, and hence of its insertion loss performance. Moreover, in literature, it has been shown that changing the physical width of the waveguide introduces a phase shift [20]. However, to improve the matching of the phase shifter proposed in [20], the authors increased the size of the waveguide rather than decreasing it, so they get better matching performance. Finally, we expect that it would be possible to improve the matching performance, of the proposed SIW phase shifter incorporating non-alternating vias, by increasing the physical width of the phase shifter, in similar manner to that reported in [20]. However, increasing the width of the waveguide will make it more difficult to integrate the proposed phase shifter within a feeding structure e.g. to realize a complete phased array antenna.

TABLE II.
SUMMARY OF THE PERFORMANCE OF PHASE SHIFTER B AT 10 GHz WITH 8 NON-ALTERNATING LM VIAS

State (S)	active LM vias	Maximum Simulated Phase Step	total phase shift	Insertion Loss (dB)
(S1)	0	NA	NA	1.6
(S2)	1	30.5°	30.5°	2.4
(S3)	2	35.4°	65.9°	1.7
(S4)	3	29.5°	95.4°	2.2
(S5)	4	40°	135.4°	2.4
(S6)	5	26.3°	161.7°	2.1
(S7)	6	38.3°	200°	2.5
(S8)	7	32.1°	232.1°	3.2
(S9)	8	33.1°	265.2°	3.5
	Total		265.2°	

C. Phase Shifter C with 10 non alternating LM via

Phase shifter C is designed based on using ten non-alternating vias with a phase step of 36° . This is mainly to improve the bandwidth (BW) and insertion loss performance of the phase shifter with eight LM vias.

In fact, it would be possible to improve the BW of the proposed phase shifter with non-alternating vias by more than 20% in all operating states by designing a new phase shifter having a phase steps less than 45° . The phase shifter is shown in Fig. 1(c). Reducing the phase step to 36° by moving the LM via away from the center of the SIW ($m = 3.5$ mm) improves the matching and the 3dB cut off frequency of the phase shifter for all operating states, as shown in Fig. 5. In more detail, the 3dB cut off frequency ranges from 9.1 GHz to 9.6 GHz for all operating states, except State 2 which has a 3dB cut off frequency of 8.1 GHz

and State 1 which has a 3dB cut off frequency below 8 GHz. This results in an improvement in the IL and bandwidth of the phase shifter, as shown in Fig. 5 and explained in Table III.

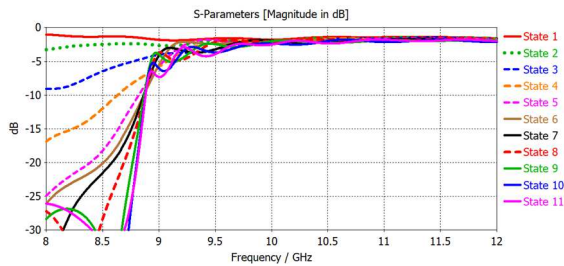


Fig. 5. Insertion loss performance of the phase shifter C with 10 alternating vias.

TABLE III.

SUMMARY OF THE PERFORMANCE OF PHASE SHIFTER C WITH TEN ALTERNATING LM VIAS

State (S)	Phase Shift (°)	IL At 10 GHz (dB)	Frequency Range
S2	36	2.2	8-12
S3	72	2.3	9-12
S4	108	2.0	9.2-12
S5	144	2.2	9.2-12
S6	180	2.1	9.2-12
S7	216	1.9	9.2-12
S8	252	2.1	9.3-12
S9	288	2	9.3-12
S10	324	2.4	9.2-12
S11	360	2.6	9.2-12

V. CONCLUSION

This paper introduces three compact phase shifters based on substrate integrated waveguide (SIW) technology, ideally suited for integration into phased array antennas. The paper outlines the design process for these phase shifters and provides simulation and experimentally verified results for a hardware prototype. The proposed phase shifters are reconfigurable using liquid metal (LM) vias. They offer a remarkable up to 360° phase-shifting range while maintaining low insertion loss. LM is utilized to create removable vias, allowing for phase reconfiguration. To activate a specific via, an LM-filled drill hole is used, and when no longer needed, the LM can be removed. Each phase shifter incorporates several holes, enabling a high phase shift. These proposed phase shifters offer several significant advantages compared to existing technology, including low IL and high power handling capability.

ACKNOWLEDGMENT

This work is funded by the United Kingdom Engineering and Physical Research Council (EPSRC) under grant number: EP/P008402/1, EP/P008402/2 and EP/V008420/1.

REFERENCES

[1] K. -J. Koh and G. M. Rebeiz, "0.13 μ m CMOS Phase Shifters for X-, Ku-, and K-Band Phased Arrays," *IEEE J. of Solid-State Circuits*, vol. 42, no. 11, pp. 2535-2546, Nov. 2007.

[2] W. Luo, H. Liu, Z. Zhang, P. Sun and X. Liu, "High-Power X-Band 5b GaN Phase Shifter with Monolithic Integrated E/D HEMTs Control Logic," *IEEE Trans. Electron Devices*, vol. 64, no. 9, pp. 3627-3633, Sept. 2017.

[3] M. Teshiba, R. Van Leeuwen, G. Sakamoto, and T. Cisco, "A SiGeMMIC 6-bit PIN diode phase shifter," *IEEE Microw. Wireless Compon. Lett.*, vol. 12, no. 12, pp. 500-501, Dec. 2002.

[4] Z. Li, J. Qiao and Y. Zhuang, "An X-Band 5-Bit Active Phase Shifter Based on a Novel Vector-Sum Technique in 0.18 μ m SiGe BiCMOS," *IEEE Trans. on Circuits and Sys. II: Express Briefs*, vol. 68, no. 6, pp. 1763-1767, June 2021.

[5] M. Sazegar *et al.*, "Low-Cost Phased-Array Antenna Using Compact Tunable Phase Shifters Based on Ferroelectric Ceramics," *IEEE Trans. Microw. Theory Techn.*, vol. 59, no. 5, pp. 1265-1273, May 2011.

[6] M. Sazegar, Y. Zheng, H. Maune, C. Damm, X. Zhou and R. Jakob, "Compact Tunable Phase Shifters on Screen-Printed BST for Balanced Phased Arrays," *IEEE Trans. Microw. Theory Techn.*, vol. 59, no. 12, pp. 3331-3337, Dec. 2011.

[7] Nahid Vahabisani, Sabreen Khan, Mojgan Daneshmand, "A K-Band Reflective Waveguide Switch Using Liquid Metal," *IEEE Antennas Wireless Propag. Lett.*, vol. 16, pp. 1788-91, Mar. 2017.

[8] Z. Qu, Y. Zhou, S. Alkaraki, J. R. Kelly and Y. Gao, "Continuous Beam Steering Realized by Tunable Ground in a Patch Antenna," *IEEE Access*, vol. 11, pp. 4095-4104, 2023.

[9] Meng Wang, Ian M. Kilgore, Michael B. Steer, Jacob J. Adams, "Characterization of Intermodulation Distortion in Reconfigurable Liquid Metal Antennas," *IEEE Antenna Wireless Propag. Lett.*, vol. 17, no. 2, pp. 279-82, Feb. 2018.

[10] J. H. Dang, R. C. Gough, A. M. Morishita, A. T. Ohta and W. A. Shiroma, "Liquid-metal-based phase shifter with reconfigurable EBG filling factor," in *Proc. IEEE MTT-S Int. Microw. Symp.*, Phoenix, AZ, 2015, pp. 1-4.

[11] Z. Qu, J. R. Kelly, Z. Wang, S. Alkaraki and Y. Gao, "A Reconfigurable Microstrip Patch Antenna With Switchable Liquid-Metal Ground Plane," *IEEE Antennas and Wireless Propagation Letters*, vol. 22, no. 5, pp. 1045-1049, May 2023.

[12] S. Alkaraki, A. L. Borja, J. R. Kelly, R. Mittra and Y. Gao, "Reconfigurable Liquid Metal-Based SIW Phase Shifter," *IEEE Transactions on Microwave Theory and Techniques*, vol. 70, no. 1, pp. 323-333, Jan. 2022.

[13] S. Alkaraki, J. Kelly, A. L. Borja, R. Mittra and Y. Wang, "Gallium-Based Liquid Metal Substrate Integrated Waveguide Switches," *IEEE Microwave and Wireless Components Letters*, vol. 31, no. 3, pp. 257-260, Mar. 2021.

[14] Y. -W. Wu, S. Alkaraki, S. -Y. Tang, Y. Wang and J. R. Kelly, "Circuits and Antennas Incorporating Gallium-Based Liquid Metal," *Proceedings of the IEEE*, vol. 111, no. 8, pp. 955-977, Aug. 2023.

[15] K. Sellal, L. Talbi, T.A. Denidni, J. Lebel, "Design and implementation of substrate integrated waveguide phase shifter," *IET Microw., Ant. & Prop.*, Vol.2, pp. 194-197, Mar. 2008.

[16] K. Hettak, G. A. Morin and M. G. Stubbs, "A novel miniature CPW topology of a high-pass/low-pass T-network phase shifter at 30 GHz," *2009 Eur. Microw. Conf. (EuMC)*, 2009, pp. 1140-1143.

[17] Y. Leviatan, P. G. Li, A. T. Adams and J. Perini, "Single-Post Inductive Obstacle in Rectangular Waveguide," *IEEE Trans. on Microw. Theory and Techn.*, vol. 31, no. 10, pp. 806-812, Oct. 1983.

[18] Young, L. Yan, W. Hong, K. Wu, and T. J. Cui, "Investigations on the propagation characteristics of the substrate integrated waveguide based on the method of lines," *IEE Proc. Microw., Antennas and Propag.*, vol. 152, no. 1, pp. 35-42, Feb. 2005. Doi:10.1049/ip-map:20040726

[19] J. E. Rayas-Sanchez and V. Gutierrez-Ayala, "A general EM-based design procedure for single-layer substrate integrated waveguide interconnects with microstrip transitions," *2008 IEEE MTT-S Int. Microw. Symp. Digest*, Atlanta, GA, USA, 2008, pp. 983-986.

[20] Y. -M. Yang, C. -W. Yuan and B. -L. Qian, "A Novel Phase Shifter for Ku-Band High-Power Microwave Applications," in *IEEE Transactions on Plasma Science*, vol. 42, no. 1, pp. 51-54, Jan. 2014.